

# Laser induced birefringence in a wavelength-mismatched cascade system of inhomogeneously broadened Yb atoms

Tai Hyun Yoon,\* Chang Yong Park, and Sung Jong Park

*Center for Optical Frequency Control*

*Korea Research Institute of Standards and Science*

*1 Doryong, Yuseong, Daejeon 305-340, Korea*

(Dated: July 22, 2004)

We report the observation of laser induced birefringence (LIB) in a wavelength-mismatched cascade system ( $J = 0 \leftrightarrow J = 1 \leftrightarrow J = 0$  transitions) of inhomogeneously broadened ytterbium atoms with strong pump and probe fields. We investigate the transmission spectrum of two circular polarization ( $\sigma_p^+$  and  $\sigma_p^-$ ) components of strong probe field at fixed frequency, depending on the detuning of circularly polarized ( $\sigma_c^-$ ) coupling field from two-photon resonance. We find that  $\sigma_p^+$  ( $\sigma_p^-$ ) polarized component exhibits a narrow electromagnetically induced absorption (transparency) spectrum. Numerical solutions of density matrix equations show qualitative agreement with experimental results. A Doppler-free dispersive LIB signal is obtained by detecting the Stokes parameter of the probe field, enabling us to stabilize the frequency of coupling laser without frequency modulation.

PACS numbers: 42.62.Fi, 32.80.Pj, 39.25.+k

Quantum coherence effects in atomic three-level systems interacting with two monochromatic laser fields provide a rich source of interesting phenomena in laser spectroscopy, for instance, the phenomena of electromagnetically induced transparency (EIT) and absorption (EIA) [1], etc. Complete coherent control of the polarization state of an optical field [2], measurement of the optical rotation to investigate the atomic parity nonconservation in thallium vapor [3], and measurement of birefringence at 1083 nm in  $^4\text{He}$  atoms [4] have been achieved relying on the EIT effects in the corresponding cascade three-level atomic systems. Recently, Magno and coworkers [5] proposed a simple scheme for laser cooling of alkaline-earth and ytterbium atoms using a two-photon  $^1S_0 \leftrightarrow ^1P_1 \leftrightarrow ^1S_0$  cascade transition, which might be used as a second stage cooling after precooling with the  $^1S_0 - ^1P_1$  transition, and this two-photon laser cooling scheme has not been realized yet experimentally.

In this paper, we present a Doppler-free two-photon atomic coherence spectroscopy of Yb atoms associated with the wavelength-mismatched cascade scheme considered in the two-photon cooling of Yb atoms [5]. We investigate the Doppler-free transmission spectrum of two circular polarization ( $\sigma_p^+$  and  $\sigma_p^-$ ) components of strong probe field at fixed detuning from one-photon resonance in a Yb hollow cathode lamp (HCL) depending on the detuning of circularly polarized ( $\sigma_c^-$ ) counterpropagating coupling field from two-photon resonance. We find that when the Rabi frequencies of the probe and coupling fields are similar to the decay rate of the  $J = 1$  state,  $\sigma_p^+$  component exhibits a narrow electromagnetically induced absorption (EIA) spectrum, while  $\sigma_p^-$  component exhibits an electromagnetically induced transparency (EIT) spectrum due the multiphoton process in-

duced via the strong probe field. The measured spectra show qualitative agreement with the calculated spectra from numerical solutions of semiclassical density matrix equations. A sensitive Doppler-free dispersive signal which is proportional to the birefringence experienced by two circular polarization components of the probe field is then subsequently obtained by detecting the Stokes parameter [6] of the transmitted probe field. This is the first measurement, as far as the authors know, of the electromagnetically induced birefringence originated from the EIA-type resonance of the strong probe field in the wavelength-mismatched three-level cascade system. Finally, we are able to stabilize the frequency of coupling laser at 1077 nm by use of the laser induced birefringence (LIB) signal with long-term stability below 1 MHz, which is stable enough to study the two-photon laser cooling of Yb atoms in a Yb magneto-optical trap (MOT) [7].

Figure 1(a) and (b), respectively, show the three-level cascade scheme of Yb atoms having  $m$ -degenerate sublevels  $|2\rangle$  and  $|3\rangle$  relevant to the present study and the schematic diagram of the experimental set-up. In Fig. 1(a), the levels  $|1\rangle$ ,  $|2\rangle$ , and  $|4\rangle$  form a three-level cascade wavelength-mismatched configuration and the level  $|2\rangle$  and  $|3\rangle$  are coupled to the ground state  $|1\rangle$  by an arbitrarily intense probe field. Here we ignore the state with  $m_J = 0$  of the  $^1P_1$  state for simplicity, but include it for the numerical calculation (see later) [8]. In parenthesis on Fig. 1(a), laser frequency, polarization state, and Rabi frequency of the driving fields are shown explicitly. The  $^1P_1$  state (levels  $|2\rangle$  and  $|3\rangle$ ) decays rapidly with decay rate  $\gamma_a = 2\pi \times 28$  MHz to the level  $|1\rangle$  and there is a weak decay channel to the  $(6s6p)^3P_1$  state via the levels  $(6s5d)^3D_1$  and  $^3D_2$  (not shown), and the  $^3P_1$  state decays to the ground state by emitting 556 nm spontaneous photons with decay rate  $2\pi \times 182$  kHz. The level  $|4\rangle$  decays predominantly to the  $^1P_1$  state with decay rate  $\gamma_b = 2\pi \times 3.0$  MHz and weakly to the  $^3P_1$  state with decay rate of  $2\pi \times 0.2$  MHz [9].

\*Electronic address: thyoona@kriss.re.kr

Note that in Yb cascade three-level configuration in Fig. 1(a), where  $\omega_p \sim 2.7 \times \omega_c$ , the effects of mismatching wavelength in the EIT spectrum in Doppler-broadened media is expected to be very strong [10], i.e., the depth of EIT dip is greatly reduced from the complete transparency as opposed to the case when  $\omega_p \simeq \omega_c$  [11] and  $\omega_c \sim 1.5 \times \omega_p$  [4]. In this case, the Autler-Townes components for nonzero velocity atoms are completely overlap with line center as oppose to the case when  $\omega_p \leq \omega_c$ , thus one would reasonably expect transparency created on resonance to be obscured [10]. This is exactly what happens in the cascade system of Fig. 1(a) and observed in Fig. 2 below, where we could detect only a few percent contrast of EIT or EIA signals against Doppler profile only when the Rabi frequencies of probe and coupling fields are an order of the decay rate of the  $J = 1$  state.

Theoretical analysis of the LIB in the same level configuration as in Fig. 1 was discussed previously by Patnaik and Agarwal [8] at the *weak* probe-field limit and wavelength *matched*-configuration, i.e.,  $\omega_p = \omega_c$ . We find, however, that in the wavelength-*mismatched* and inhomogeneously broadened cascade configuration, where  $\omega_p \gg \omega_c$  as in Ca, Sr, and Yb atoms (considered in the two-photon cooling theory [5]), the LIB signal becomes negligibly small after Doppler averaging [10] when the probe field is weak. Thus, we can not use the analytical results discussed in Ref. [8] for the explanation of our experimental findings. In this paper, we demonstrate that if the probe field is *strong* in this level configuration two circular polarization components of the probe field exhibit EIA in the  $\sigma_p^+$  component which is coupled to the control field and EIT in the  $\sigma_p^-$  component which is decoupled from the control field, allowing us to measure the laser induced birefringence originated from the EIA-type resonance. This is the first observation, as far as the authors know, of an electromagnetically induced birefringence associated with the EIA and EIT effects of the strong probe field in the cascade three-level system.

In the experiment, two laser diodes with external grating feedback are used for the probe laser (PL) and coupling laser (CL), respectively, as indicated in Fig. 1(b). The atomic temperature in a Yb HCL is estimated to be  $\sim 600$  K, which gives a Doppler width of  $\sim 1$  GHz [12]. The frequency of probe laser at 399 nm can be stabilized within the range of probe detuning  $|\delta_p| < 2\gamma_a \sim 60$  MHz by use of a Doppler-free saturation absorption signal with lock-in detection using a separate Yb HCL. Two-photon Doppler cancellation, although it is not perfect since  $\omega_p \neq \omega_c$ , is achieved with counterpropagating geometry of the coupling and probe fields as in Fig. 1(b). We set the powers of the probe and coupling fields at  $P_p = 85 \mu\text{W}$  (spot size  $67 \mu\text{m}$ ,  $\Omega_p \sim 2\gamma_a$  for  $\sigma_p^+$  and  $\sigma_p^-$  components) and  $P_c = 1.7 \text{ mW}$  (spot size  $175 \mu\text{m}$ ,  $\Omega_c \sim 4\gamma_a$ ), and the probe field detuning at exact one-photon resonance ( $\delta_p = 0$ ).

We first measured the transmittance spectrum corresponding to the two circularly polarized components of the probe field as a function of coupling field detuning

$\delta_c/\gamma_a$ . For this measurement, we used two detectors (PD1 and PD2) in Fig. 1(b) and a  $\lambda/4$  wave-plate oriented at  $45^\circ$  to the PBS. The first column in Fig. 2 shows the typical transmission spectrum expressed as a contrast against Doppler background (70 % absorption) corresponding to the  $\sigma_p^-$  component in (a) and to the  $\sigma_p^+$  component in (b) for the  $^{174}\text{Yb}$  isotope in a Yb HCL with Ne buffer gas (discharge voltage 160 V and current 1.8 mA) [7]. As one can see, the spectrum in (a) corresponds to the  $\sigma_p^-$  component shows an EIT spectrum with a line width of  $\sim 3\gamma_a$ , while the spectrum in (b) corresponding to the  $\sigma_p^+$  component shows a narrower ( $\sim \gamma_a$ ) EIA spectrum at the two-photon resonance. Note that the EIT and EIA spectrum has only a few percent contrast against Doppler background, which is expected theoretically for the wavelength-mismatched cascade system with  $\omega_p \gg \omega_c$  [10]. We also find that, as decreasing the intensity of coupling field, the EIA spectrum in (b) develops into the EIT spectrum as in (a) with reduced signal-to-noise ratio. However, the  $\sigma_p^-$  component which is decoupled from the strong control field exhibits always an EIT spectrum under the parameter range we have tested. The EIT spectrum has a line width about 87 MHz  $\sim 3\gamma_a$ , which is 1.5 times larger than the width measured at the Doppler-free saturation absorption spectroscopy with a same Yb HCL due to the saturation broadening [7], while the EIA spectrum has much narrow line width about  $\gamma_a$ . We calibrated the width of the measured spectrum from the known frequency interval (isotope shift) of the  $^1S_0 - ^1P_1$  transition of Yb isotopes [13]. The narrow feature of the EIA spectrum may be understood that in the EIA process higher order multi-path interference is involved compared to the EIT process, since the probe field is strong [11].

In order to understand theoretically the measured spectra in Fig. 2(a) and (b), we solved a semiclassical density matrix equation associated with the level configuration of Fig. 1(a) at the steady state. The equation of motion for the slowly varying components  $\rho$  of the density matrix  $\tilde{\rho}$  may be written by making a transformation  $\tilde{\rho} \rightarrow \rho$  such that  $\rho_{kk} = \tilde{\rho}_{kk}$ ,  $\rho_{11} = \tilde{\rho}_{11} \exp(-i\omega_p t)$ ,  $\rho_{4l} = \tilde{\rho}_{4l} \exp(-i\omega_c t)$ ,  $l = 2, o, 3$ ,  $\rho_{41} = \tilde{\rho}_{41} \exp[-i(\omega_p + \omega_c)t]$ , where subscript "o" indicates the state with  $m = 0$  of the  $^1P_1$  level. The matrix equation for  $\rho$  is then found to be [8]

$$\dot{\rho} = -\frac{i}{\hbar}[H, \rho] - \sum_{i=2,o,3} (\gamma_b/6\{|4\rangle\langle 4|, \rho\} + \gamma_a/2\{|i\rangle\langle i|, \rho\} - \gamma_b\rho_{44}|i\rangle\langle i| - \gamma_a\rho_{ii}|1\rangle\langle 1|), \quad (1)$$

with the effective hamiltonian in the rotating frame

$$H = \hbar(\delta_p + \delta_c)|4\rangle\langle 4| + \hbar\delta_p \sum_{i=2,3} |i\rangle\langle i| - \frac{\hbar}{2} \sum_{i=2,3} (\Omega_p|i\rangle\langle 1| + \Omega_c|4\rangle\langle 2| + \text{h.c.}). \quad (2)$$

The second term under the summation sign of Eq. (1)

represents the natural decays of the system and the curly bracket represents the anti-commutator.

The second column in Fig. 2 ((c) and (d)) shows the calculated transmission spectrum of the probe field after Doppler averaging expressed as a contrast against Doppler background as a function of  $\delta_c/\gamma_a$  with the parameters  $\Omega_p = \Omega_c = 2\gamma_a$ . The calculated contrast of the probe field transmittance against Doppler background was obtained from the imaginary part of the atomic coherence, i.e.,  $\text{Im}[\rho_{31}]$  for  $\sigma_p^-$  component and  $\text{Im}[\rho_{21}]$  for  $\sigma_p^+$  component. The spectrum in (c) shows an EIT spectrum as in (a), while the spectrum in (d) corresponding to the  $\sigma_p^+$  component shows an EIA spectrum as in (b) at the same parameters. The EIA spectrum of the  $\sigma_p^+$  component of the probe field can be understood as a result of higher-order multiphoton interference enabled by the strong probe field [11]. In addition, our experimental and numerical observations suggest that the  $\sigma_p^-$  component which is blind to the coupling field is also actually strongly coupled to the  $\sigma_c^-$  coupling field due to the multiphoton process induced via the strong probe field so that the EIT spectrum is observed.

Although, as one can find, the experimental and theoretical spectra in Fig. 2 agree well qualitatively, there are significant difference in line shape. We attribute this difference partly to the unknown discharge effects in the Yb hollow-cathode lamp and partly to the uncontrollable imperfections of the polarization elements in the experimental set-up. However, we can reasonably say that the density matrix equations in Eqs. (1) and (2) correctly describes the general behavior of the atomic coherence associated with the three-level cascade system with  $m$ -degenerate sublevels in Fig. 1(a). We want to emphasize that at the parameter range where  $\Omega_p \ll \gamma_a$  and  $\Omega_c \sim \gamma_a$ , the calculated transmittances for both  $\sigma_p^+$  and  $\sigma_p^-$  components exhibit white (flat) spectrum after the Doppler averaging, thus there is no detectable EIT or EIA signals as contrary to the case when  $\Omega_p \sim \Omega_c \sim \gamma_a$  as in Fig. 2, supporting strongly our observations. Therefore it is very important experimental and theoretical observation that only when the intensity of the probe field and coupling fields are strong, i.e.,  $\Omega_p \sim \Omega_c \sim \gamma_a$ , the transmittances of the  $\sigma_p^+$  and  $\sigma_p^-$  components in the wavelength-mismatched cascade system exhibit an enhanced absorption or transmittance induced by the narrow two-photon coherence, resulting in the enhancement of laser induced birefringence as clearly demonstrated in Fig. 3(a) below.

Strong coupling and probe fields, when applied to an initially isotropic medium containing Yb atoms having  $m$ -degenerate sublevels, can create birefringence in the medium. Because, as clearly seen in Fig. 2, the strong driving fields create asymmetry between the susceptibilities  $\chi^\pm$  of the probe field, since  $\chi^{+(-)} = (2\mu/\epsilon_0 E_p) \rho_{21(31)}$ , where  $\mu$  is the dipole matrix element between  $^1S_0 - ^1P_1$  transition,  $\epsilon_0$  is the permittivity, and  $E_p$  is the amplitude of the probe field. That results in the LIB, i.e, the plane of polarization is rotated when it

passes through the medium. For a small absorption the rotation angle  $\Delta\theta$  is given by [6, 8]

$$\Delta\theta = \pi k_p L (\chi^+ - \chi^-) = \Delta n k_p L / 2, \quad (3)$$

where  $k_p$  corresponds to propagation vector of the probe field,  $L$  is length of the cell along  $k_p$ ,  $\Delta n = n^+ - n^-$ ,  $n^\pm + i\alpha^\pm = \sqrt{1 + 4\pi\chi^\pm}$ , and  $n^\pm$  ( $\alpha^\pm$ ) being the refractive index (absorption coefficient). Using the numerical solutions for  $\chi_p^\pm$  from Eqs. (1) and (2), the rotation of polarization  $\Delta\theta$  of the probe can easily be determined from Eq. (3). In order to detect the background-free dispersive LIB signal experimentally, we used the SPD in Fig. 1(b). In this case, the SPD consists of a  $\lambda/2$ -wave plate and a balanced polarimeter [6]. The conventional way to measure the polarization state after passing through the medium is to put a linear polarizer in front of a detector and measure the projected intensity. But, in that case, it is inevitable to include the effect of circular dichroism in addition to the rotation of the polarization axis. In the SPD scheme, however, the  $\lambda/2$ -wave plate rotates the polarization axis of the probe beam by  $45^\circ$ , and the balanced detector (polarimeter) which subtracts the reflected and transmitted intensities from the PBS measures only the rotation of the polarization axis, i.e., the LIB signal which is linear in  $\Delta\theta$  without background as long as  $\Delta\theta \ll 1$  for optically thin sample, where  $\alpha L \ll 1$  [6].

Figure 3(a) shows the detected LIB signal at the same parameter condition as in Fig. 2. The LIB signal has two distinct features originated from the absorption (dispersion) spectrum of the  $\sigma_p^+$  and  $\sigma_p^-$  components. The narrow dispersion feature at the line center with line width about  $\sim \gamma_a$  corresponds to the LIB associated with the EIA signal observed for the  $\sigma_p^+$  component in Fig. 2(b), while somewhat broad ( $\sim 3\gamma_a$ ) and weak dispersion signal superimposed on the main LIB signal corresponds to the LIB associated with the EIT signal observed for the  $\sigma_p^-$  component in Fig. 2(a). Therefore, we demonstrated for the first time the measurement of electromagnetically induced birefringence originated from the EIA-type resonance of the strong probe field in the wavelength-mismatched three-level cascade system.

Finally, we used successfully the measured dispersive LIB signal in Fig. 3(a) for the frequency stabilization of the coupling laser without frequency modulation with long-term stability below 1 MHz as shown in Fig. 3(b). Furthermore, by stabilizing the frequency of probe laser to the different isotope of Yb atoms, for example  $^{171}\text{Yb}$ , which is a promising candidate for future optical lattice clock [7, 14], we were able to stabilize the frequency of coupling laser to each stable Yb isotope. The two-photon cooling theory predicts that the minimum temperature of 124  $\mu\text{K}$  for Yb atoms can be reached at the probe and coupling laser detunings of  $\delta_p = -\gamma_a/2$  and  $\delta_c = -\gamma_b/2$  [5], respectively, those conditions can easily be achieved with the current frequency-stabilized laser diodes described in this paper.

In summary, we introduced a Doppler-free two-photon

atomic coherence spectroscopy of Yb atoms in a Yb hollow cathode lamp associated with the wavelength-mismatched cascade level configuration. We investigated the transmission spectrum of strong probe field at fixed one-photon frequency, depending on the detuning of circularly polarized coupling field from two-photon resonance. We found that  $\sigma_p^+$  polarized component which is coupled to the upper state exhibits a narrow EIA spectrum, while  $\sigma_p^-$  polarized component exhibits an EIT spectrum. Numerical solutions of density matrix equations show qualitative agreement with the experimental results. A Doppler-free dispersive LIB signal results from

the EIA-type resonance was obtained for the first time by detecting the Stokes parameter of the probe field, enabling us to stabilize the frequency of coupling laser without frequency modulation. The Doppler-free two-photon atomic coherence spectroscopy introduced in this paper might equally be applied to the alkaline-earth atoms and should be useful for experimental realization of the two-photon cooling theory [5].

This research is supported by the Creative Research Initiatives Program of the Ministry of Science and Technology of Korea. The authors thank H. S. Moon for useful discussions.

- 
- [1] K.-J. Boller, A. Imamoglu, and S. E. Harris, Phys. Rev. Lett. **66**, 2593 (1991); A. M. Akulshin, S. Barreiro, and A. Lezama, Phys. Rev. A **57**, 2996 (1998).  
 [2] S. Wielandy and A. L. Gaeta, Phys. Rev. Lett. **81**, 3359 (1998).  
 [3] A. D. Cronin, R. B. Warrington, S. K. Lamoreaux, and E. N. Fortson, Phys. Rev. Lett. **80**, 3719 (1998).  
 [4] F. S. Pavone, G. Bianchini, F. S. Cataliotti, T. W. Hänsch, and M. Inguscio, Opt. Lett. **22**, 736 (1997).  
 [5] W. C. Magno, R. L. Cavasso Filho, and F. C. Cruz, Phys. Rev. A **67**, 043407 (2003).  
 [6] C. P. Pearman, C. S. Adams, S. G. Cox, P. F. Griffin, D. A. Smith, and I. G. Hughes, J. Phys. B **35**, 5141 (2002); Y. Yoshikawa, T. Umeki, T. Mukae, Y. Torii, and T. Kuga, Appl. Opt. **42**, 6645 (2003); A. Ratnapala, C. J. Vale, A. G. White, M. D. Harvey, N. Heckenberg, and H. Rubinsztein-Dunlop, arXiv:physics/0405113.  
 [7] C. Y. Park and T. H. Yoon, Phys. Rev. A **68**, 055401 (2003).  
 [8] A. K. Patnaik and G. S. Agarwal, Opt. Commun. **199**, 127 (2001); *ibid* **179**, 97 (2000).  
 [9] Y. S. Bai and T. W. Mossberg, Phys. Rev. A **35**, 619 (1987).  
 [10] J. R. Boon, E. Zekou, D. McGloin, and M. H. Dunn, Phys. Rev. A **59**, 4675 (1999).  
 [11] S. Wielandy and A. L. Gaeta, Phys. Rev. A **58**, 2500 (1998).  
 [12] C. Y. Park and T. H. Yoon, Jpn. J. Appl. Phys. **42**, L754 (2003); J. I. Kim, C. Y. Park, J. Y. Yeom, E. B. Kim, and T. H. Yoon, Opt. Lett. **28**, 245 (2003).  
 [13] T. Loftus, J. R. Bochinski, and T. W. Mossberg, Phys.

- Rev. A **63**, 053401 (2001).  
 [14] S. G. Porsev, A. Derevianko, and E. N. Fortson, Phys. Rev. A **69**, 021403(R) (2004).

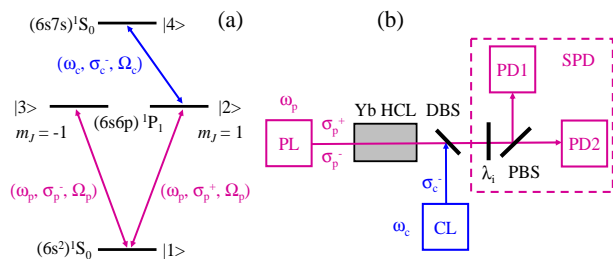


FIG. 1: (a) The three-level cascade scheme of Yb atoms having  $m$ -degenerate sublevels  $|2\rangle$  and  $|3\rangle$ . In parenthesis, laser frequency, polarization state, and Rabi frequency of the driving fields are explicitly shown. (b) Experimental set-up for Doppler-free two-photon atomic coherence spectroscopy. PL; probe laser, CL; coupling laser, SPD; Stokes parameter detector, PD; photo-diode, PBS; polarization beam splitter, DBS; dichroic beam splitter, HCL; hollow cathode lamp,  $\lambda_i$ ;  $\lambda/i$  wave-plate ( $i = 2, 4$ ).

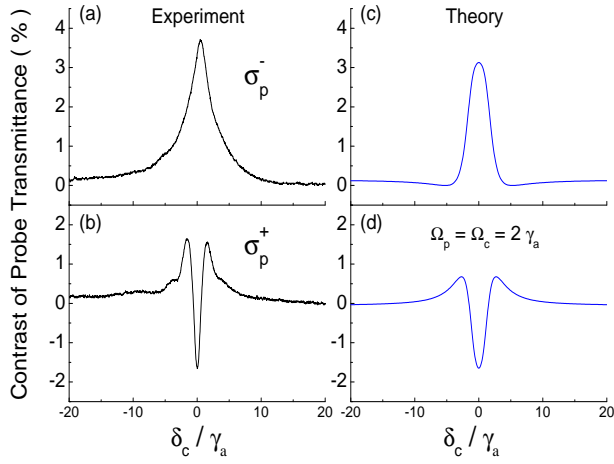


FIG. 2: Measured contrast against Doppler background of the strong probe field transmittance for  $\sigma_p^-$  (a) and  $\sigma_p^+$  component (b) versus  $\delta_c/\gamma_a$  at probe and coupling powers of  $85 \mu\text{W}$  and  $1.7 \text{ mW}$ , respectively. The graphs in (c) and (d) are, respectively, the calculated contrasts against Doppler background of probe transmittance for  $\sigma_p^-$  and  $\sigma_p^+$  component with the parameters of  $\Omega_p = \Omega_c = 2\gamma_a$ . In all graphs, we set  $\delta_p = 0$ .

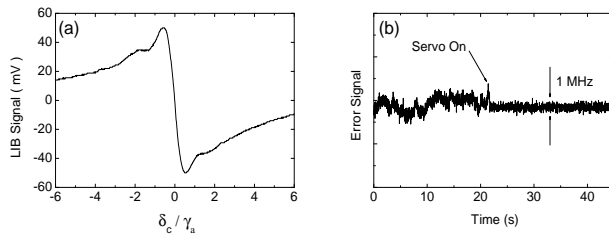


FIG. 3: (a) Doppler-free dispersive LIB signal measured by the SPD in Fig. 1(b). (b) Frequency fluctuation of the coupling laser before and after the servo-loop is on for frequency stabilization.